PIPELINE STAGE DESIGN OPTIMIZATION FOR INCREASED OPERATING RANGE

by

Gilles Nawrocki

Senior Design Engineer

GE Oil & Gas

Le Creusot, France

Denis Guenard

Aerodynamics Development of Centrifugal Compressors

and

Vittorio Michelassi

Manager of Aerodynamics

GE Oil & Gas

Florence, Italy

Gilles Nawrocki is a Senior Design Engineer for GE Oil & Gas, in Le Creusot, France. He has been working for nine years on aero-optimization of inlet/outlet and pipeline stages of centrifugal compressors. He has 17 years of experience in CFD design for the turbomachinery, nuclear energy, and automotive industries.

Mr. Nawrocki has an Engineering diploma (Aeronautics and Space Engineering) from SUPAERO Toulouse in France.

Denis Guenard is responsible for Aerodynamics Development of Centrifugal Compressors for GE Oil & Gas, in Florence, Italy. He has 13 years of experience in the field of turbomachinery and specifically centrifugal compressors, and has led design activities for many stage families currently in service in Oil & Gas.

Mr. Guenard has a DEA (Fluid Mechanics) and an Engineering diploma (Aeronautics Engineering) from ENSICA Toulouse in France.

Vittorio Michelassi is the Manager of Aerodynamics at GE Oil & Gas, in Florence, Italy. His team is responsible for aerodynamic design of axial and radial turbomachines, performance prediction, and performance database for centrifugal compressors.

Dr. Michelassi received his Engineering degree in 1984, his Ph.D. degree in 1990 from the University of Florence, and a Masters degree in 1985 from the Von Karman Institute for Fluid Dynamics in Bruxelles. He has authored nearly one hundred papers on CFD, aerodynamics, and turbomachinery.

ABSTRACT

With the continuing increase in energy demand, pipeline compressors are being challenged to cope with both large flow rates and broad operating range flexibility, driven by the local seasonal markets. Overall, high efficiency still needs to be maintained, as compressor efficiency will significantly impact on gas transportation cost. Those joint requirements call for significant improvements in pipeline compressor stage design.

This intends to highlight the experience gained in the development of these challenging stages in a unique effort combining experimental and computational fluid dynamics (CFD) studies. In particular, the study started with the detailed testing of a conventionally designed stage. Careful comparison of CFD versus test results was followed by intensive activity coordinating between CFD and testing.

The intent of those simulations was to identify the limits of this initial design and to indicate the guidelines for improvement.

The massive use of state-of-the-art CFD allowed investigations on a large number of impeller configurations. Analysis of the numerical results suggested the possibility of significant operating range improvement with minimal penalty on efficiency and choke limit.

An intensive experimental test campaign confirmed the validity of the new impeller design for improved operating range improvement but also highlighted the balance between efficiency and operating range requirements. A final optimization on a statoric component is then performed to get back to original efficiency while retaining increased operating range.

INTRODUCTION

The natural gas transportation market specifications lead to the following usual characteristics for pipeline compressors:

- Stage numbers ranging from one to three with the possible use of relatively smaller shaft diameters and of stages with higher pitch compared to upstream or downstream units
- Molecular weight of gas with minor variation leading to normal tip Mach numbers around 0.5
- Flow coefficient usually selected in the range of flow coefficient from 0.03 to 0.13 usually with a 3D impeller (2D impeller could be applied for lower flow coefficients)
- Possibility of using either vaneless or vaned diffuser configuration, depending on the relative importance of peak efficiency versus operating range
- Variable speed unit

In general, more complex features that could further increase operating flexibility, such as adjustable inlet guide vanes, are not used, even for single stage units.

This study initiated from standard pipeline stages available in the late 90s here referred to as “first generation.” This first generation was designed with traditional tools, design criteria, and

practices available at the time (mainly 1D correlations, meridional, and blade to blade analyses were used) and also derived from most successful "design on purpose" units available at the time, i.e., machines tested in the mid 90s. Test programs were followed by intensive standardization work.

From experimental validation of the first generation stages, the main conclusions were that efficiency and head coefficient at the design point were well aligned with expectation. Operation at flow higher than design was also satisfactory. On the contrary, going toward surge, behavior of the stages was not as good as expected especially for the range of design flow coefficients above 0.06. Experiments indicated that the surge limitation was due to impeller behavior. New specifications were issued targeting significant operating range increase, per market requirements, while maintaining efficiency and head.

A first level of optimization with CFD and tests was performed in 2003/2004 leading to creation and introduction of a second generation of stages with significantly improved range. However, detailed analyses of the experimental results revealed the possibility for further improvements.

After verification of coherence between experiments and CFD, an extensive CFD redesign campaign was performed using design of experiment (DOE) methodology (NIST/SEMATECH, 2003) and parametric studies. This led to a redesign for a third generation of impellers and to an optimization of the return channel. Detailed single stage tests are available on the three generations of impellers and optimized return channel is under final testing.

This paper covers essential results obtained in impeller redesign for all three generations, both from numerical and experimental point of views. Results presented here are mostly based on a design flow coefficient of 0.095 (Φ_{design}), but have been extended and experimentally confirmed for the whole range of flow coefficients from 0.06 to 0.13.

NEW DESIGN SPECIFICATIONS

Considering a 3D impeller with a diameter of 20.472 inches, a design Mach number of 0.50, and a design flow coefficient of 0.095, the following requirements (summarized in Figure 1) have been defined:

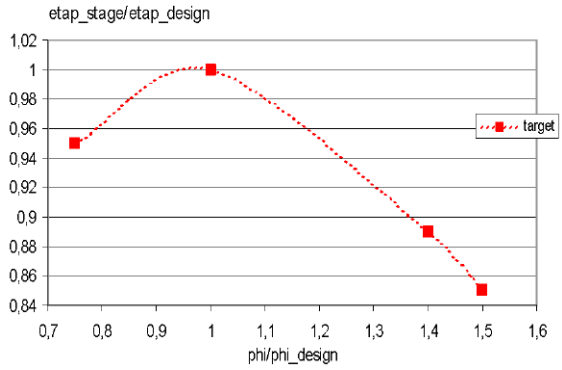

Figure 1. Normalized, Efficiency Curve Target.

- Stage peak polytropic efficiency unchanged compared to first stage generation
- Operating range from 75 to 150 percent of design flow coefficient at nominal speed
- Efficiency decrement, from peak value, of 5 percent at 75 percent of design point
- Efficiency decrement, from peak value, of 12 percent at 140 percent of design point
- Efficiency decrement, from peak value, of 15 percent at 150 percent of design point

For low Mach stages where the efficiency curve drops smoothly at high flow, a 12 percent decay of efficiency versus nominal point is conventionally taken as the upper limit (Φ_{right}), while the last stable point at low flow will be the left limit (Φ_{left}). Therefore, one can synthesize demand into overall range (OR) > 0.87 (87 percent) with overall range defined as:

$$OR = \frac{\Phi_{right}}{\Phi_{left}} - 1 \quad \textbf{(1)}$$

BASELINE—FIRST GENERATION DESIGN

The baseline design is a shrouded 3D impeller, ruled surface type, design with 17 plain blades for the impeller and 16 deswirl vanes for the return channel. In Figure 2 left, a comparison is done between this pipeline stage and a standard 3D stage. It can be appreciated that both diffuser size and axial span of the impeller have been increased in order to maximize efficiency. On the right in Figure 2 is a view of the impeller with cover removed. The original deswirl vane blade type is of the same type as for any other stage with no specific optimization.

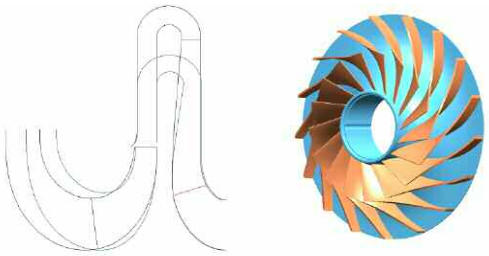

Figure 2. Baseline Design, Cross-Section Superimposed with Standard Stage and 3D, Unshrouded Model.

In the present study, a vaneless diffuser configuration has been used to obtain better operating range. Vaned diffusers can be used to maximize peak efficiency with reduced diffuser size but with significant impact on range.

Original design of first generation impellers was done only with the help of 1D correlations and combination of meridional and blade-to-blade calculations. From the 1D code, the choice was made for the aerodynamic design parameters such as tip deceleration, design incidence angle, number of blades, and estimated leading and trailing edges' angles.

From the meridional (streamline curvature method) and blade-to-blade (vorticity conservation method), verification is done for leading edge incidence. Blade detailed design is done in order to match a targeted relative velocity distribution, distribution thought to be optimal for the given relative Mach number. A classical loading diagram can be found from different authors (Aungier, 2000; Japikse, 1996) and, of course, will depend on each manufacturer's know-how. For low relative Mach number, common practice is to start to load the impeller blade rather rapidly at the leading edge, where the boundary layer is still reduced, and to unload at the trailing edge to reduce mixing losses (Dallenbach, 1961; Nishida-Nishina, 1983).

Hub design follows the same type of criterion with the exception that it is normally considered less critical from the aerodynamic point of view. In most cases, hub design will be more twisted, with a classical S shape. This is done to achieve a blade nearly radial at the leading edge, with a low rake angle at the trailing edge both for mechanical reasons and to optimize impeller machining.

While this approach does provide solid guidelines for the designer in terms of general pattern for a relative speed diagram, it does not allow a full appreciation of the consequences of different local loading on stage performances. Moreover, simplified blade-to-blade tools have often limited accuracy specifically close to leading or trailing edges.

First Generation Test Results

The complete stage (impeller, vaneless diffuser and return channel) was tested using a research and development (R&D) experimental rig and considering an intermediate stage configuration (Figure 3). A standard list of instrumentation at different sections is listed in Table 1. In some tests, two sections 00 and 41 have been added but were not present in the baseline.

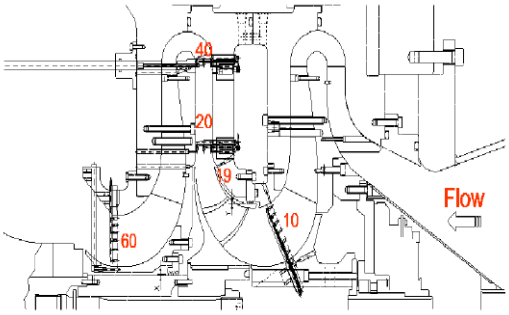

Figure 3. Typical View of Test Rig and Definition of Different Sections.

Table 1. Standard Instrumentation List.

	00	10	19	20	40	41	60
Tangential traversing	Y	Y					
Kiel Rakes	1/5			4/1		2/2	
Thermocouple Rakes	1/5					2/1	4/3
Traw. Thermocouples				2			
Cobra Rakes	5	6		1			2/3
3FM							4/4
Wall Taps (hub)	4	2	4	4	4		4
Wall Taps (shroud)	4	4	4	4	4		4
PCBs				2	2		

A pseudo stage is defined upstream of the measured stage with preswirl and deswirl vanes. They are designed to deliver mean flow angle and flow distortions similar to a real stage at design point only. In some tests, preswirl and deswirl vanes can be removed to assess effect of different inlet conditions.

Depending on the number of blade/vane rows modeled by CFD, the following terminology is used in the rest of this paper:

- *1af*—One airfoil computation with impeller and vaneless diffuser
- *2af*—Two airfoil computation with impeller, vaneless diffuser, and deswirl vane/return channel
- *4af*—Four airfoil computation to perform numerical investigation with all vanes/blades as for the test rig

Similar test conditions have been used with respect to design Mach number of 0.50 and design flow coefficient of 0.095 as the tested impeller has a diameter of 17.717 inches.

- Air at atmospheric pressure and 527 Rankine
- 7290 rpm at nominal speed

Even though the major objective is the determination of overall stage performances, effort was made to get information on losses for each element, impeller, diffuser, or return channel, with the help of intermediate measurements. Left limit for the stage, of key importance for the present study, is determined to be the onset of either of two phenomena: flattening of the polytropic head curve or the appearance of pressure pulsations (sub- rarely hyper-synchronous) linked to rotating stall on any component.

In all graphs, polytropic head coefficient is referred to as TauEtap, while Etap is the polytropic efficiency given in normalized form:

$$Tau = \frac{\Delta Ht_{60-10}}{U^2}; \qquad TauEtap = Tau * Etap \tag{2}$$

where Ht and Etap refer, respectively, to specific total enthalpy of fluid and polytropic efficiency calculated between section 10 and 60.

Normally, if the first phenomenon encountered is subsynchronous vibration, the stall flow coefficient can be determined with an absolute precision equal to the precision of the flow measurement (around 2 percent). While in the case of flattening of the head curve, the determination of the left limit is somewhat imprecise. In most of the cases on the R&D test bench, however, it is found that the pressure pulsations appear before or at the same position as the onset of the flattening of the head curve.

Figure 4 gives the results obtained with the first generation. A zero slope of TauEtap coefficient characterizes surge limit and at the same location (89 percent of design) subsynchronous pressure pulsations were measured. Interestingly, it can be seen that those pressure pulsations do appear while the stage is nearly at maximum efficiency.

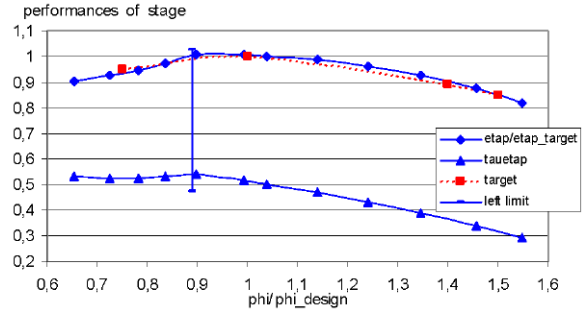

Figure 4. Performances of Baseline.

It is worthwhile noting that the design point here is the one originally intended by the designer. From a practical point of view, this stage would be selected at 110 or 115 percent of its design flow in order to maintain sufficient margin to stall. This, of course, will not change the global operating range of the stage and is valid only if the global operating range is acceptable. Pressure pulsations had a frequency of 85 percent of rotational speed, typical of impeller stall phenomenon.

To even better isolate the source of this left limit and identify a possible component interaction between impeller with either upstream return channel or downstream vaneless diffuser, two additional tests were run. The first was performed by removing the two rows of blades upstream of the impeller (Figure 5, curve B), the second by installing a low solidity vaned diffuser (Figure 5, curve C).

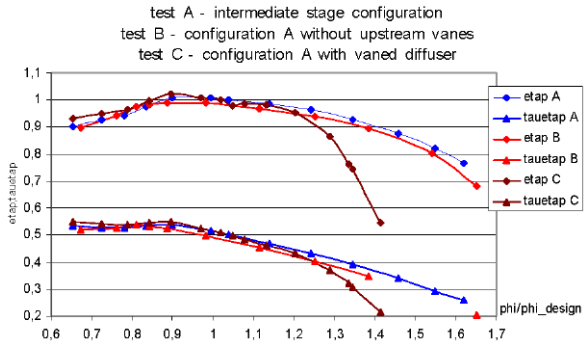

Figure 5. Modified Stators Tests.

The overall left limit remained unchanged with test C indicating: from the slight shift of TauEtap curve that the original impeller is operating with some counter rotation from upstream. This element is something that is not desired for aerodynamic optimization and will therefore be addressed in return channel optimization. The simple conclusion from those tests was that left limit was only driven by impeller and very likely from its leading edge zone.

In parallel with experimental measurements, this stage was used to calibrate the CFD methodology and assess its predictability capacity. From the indication of the test results, the focus was placed on the impeller and a limited computational domain was used with uniform boundary conditions at the inlet of the domain.

This CFD study was performed with both commercial software and an internal software. Typical grid topology used is of O-H type (Figure 6) with K-ω or K-ε high Reynolds turbulence models; boundary layers are computed according to wall function hypotheses.

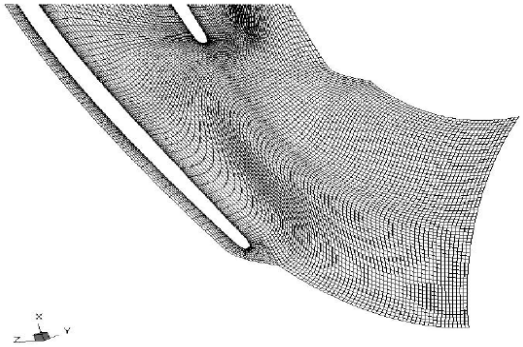

Figure 6. O-H Meshing Domain for Internal Software.

Overall, in this first version and despite the simplification of domain and boundary conditions, all software captured left limit with good accuracy (Figure 7), and all, as expected, indicated inception of impeller stall at shroud (Figure 8). To be more precise, stall zone appears close to leading edge where meridional turning of the flow begins.

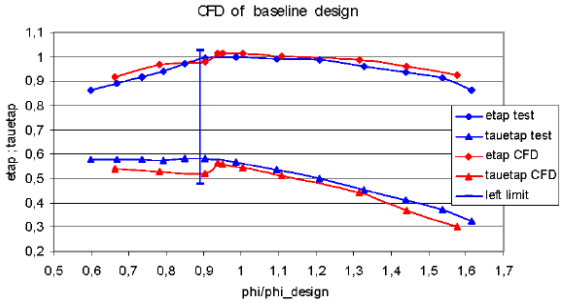

Figure 7. CFD Analysis of Baseline Impeller, Overall Comparison of Performance Curves.

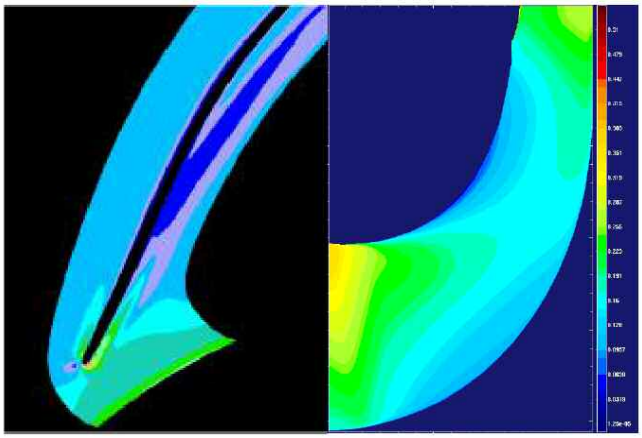

Figure 8. Relative Mach Number at Last Monotonous Convergence Point.

Studies continued with intensive CFD use, the objective of which was to indicate guidelines for improvement. From those first studies, a certain number of parameters were identified and used to create an optimization plan.

At a first level both from the result of test, CFD, and also from conventional aerodynamic practice, it was decided to focus on the shroud design. Figures 8 and 9 give a qualitative explanation for the choice not to modify actual incidence of the impeller. In fact, from CFD, no incidence problem was identified but more a load problem where both strong blade and meridional curvatures are present. In all subsequent steps of optimization, the stall mechanism remained quite similar even though at different flow coefficient.

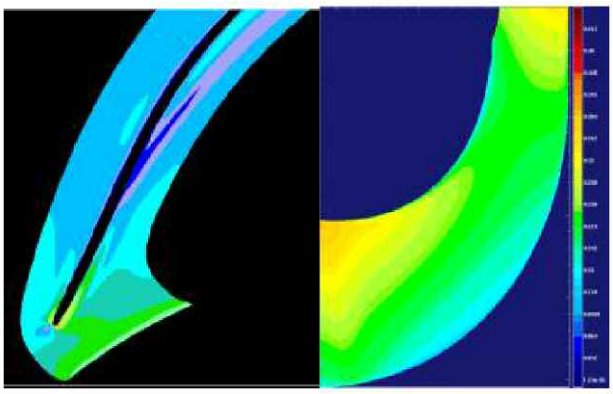

Figure 9. Relative Mach Number at Design Point.

SECOND GENERATION OF STAGES

DOE Based Optimization—Methodology

In view of the good results provided by numerical computations, a CFD based DOE was considered to optimize the baseline in order to maintain design and choke performances and improve surge limit. This type of optimization has been successfully used in the past for other designs (Bonaiuti, et al., 2006).

Definition of Parameters

As blades are defined considering ruled surfaces, geometry at the shroud is fully defined by three curves as shown on Figure 10:

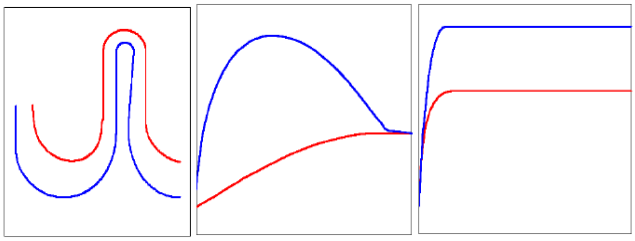

Figure 10. Meridional View, Blade Angle Evolution and Thickness Law at Shroud.

- Meridian cross section (parameter 1),
- Beta metal angle distribution (parameter 2),
- Thickness distribution (parameter 3).

Each curve is a spline defined by many control points that are the real basic parameters. To take into account all possible variations would induce an unacceptably large DOE. The three main parameters are then considered for the DOE with three discrete curves using conventional variation. Value 0 refers to baseline curve, −1 and +1 to two extreme positions. Evolution of control points' positions is considered linear between each level. Levels −1 and 1 are symmetric with respect to baseline as shown in Figure 11 for blade angle distribution.

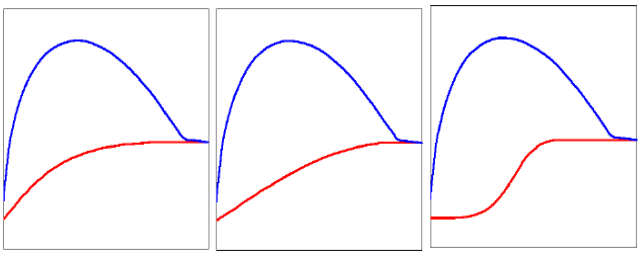

Figure 11. "Discrete Data" Curve for Blade Angle from Left to Right, Typical Shape for Levels −1/0/+1.

Finally, this simplified DOE can be considered as an optimization of leading edge for the mean following parameters:

- Blade camber
- Leading edge shape
- Meridional curvature

First Level—Shroud DOE Optimization

Using Box-Behnken response surface, 15 CFD runs were defined to perform a factorial DOE. Quick presentation of Six-Sigma and DOE techniques can be found from NIST/SEMATECH (2003). From this surface, a simple fit has been extracted on the optimum efficiency line that allows one to link more directly efficiency decay at design with operating range variation as shown in Figure 12.

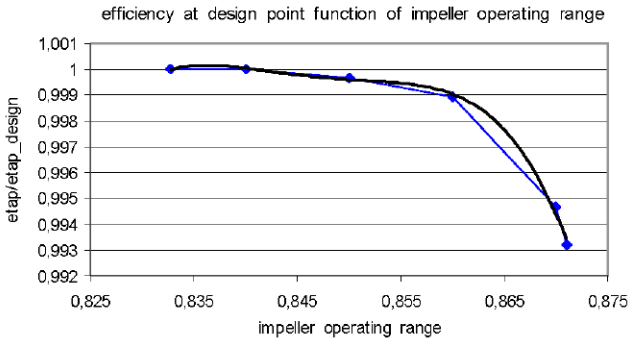

Figure 12. Impeller Operating Range Function of Design Efficiency from CFD.

Polytropic efficiency is computed between impeller inlet and vaneless diffuser inlet. Operating range is defined by the following formula:

- *Left limit CFD*—When the code does not converge
- *Right limit*—Where $\eta = \eta_{design} * 0.88$
- *Impeller operating range (IOR)*—$(\Phi_{right} - \Phi_{left})/\Phi_{design}$

It must be noted that, in this case, the definition of operating range is from the CFD of the impeller plus diffuser. Results are not exactly the same for a full stage and, therefore, variation of operating range must be taken in a relative way.

A good balance between efficiency and operating range is to a normalized efficiency of 0.999 and an increase of IOR of 4 percent. The result achieved by DOE showed a possible improvement of 8 percent of the left limit for the stage operating range still maintaining performances at design point and identical right limit as shown by Figure 13.

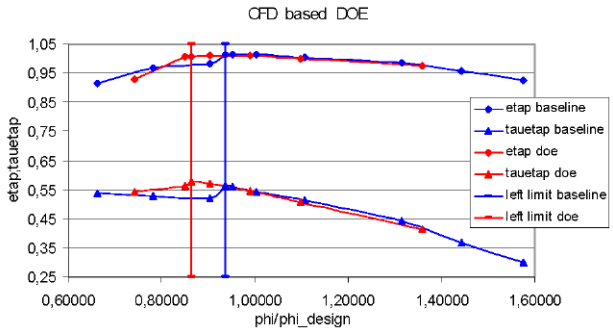

Figure 13. CFD Based DOE.

First Level DOE—Experimental Validation

Using stationary components from the initial experimental test and four airfoil configurations to reproduce the intermediate stage configuration, an experimental validation of the optimized impeller was performed. The design point performances are actually maintained while an improvement of 11.5 percent is found on the left limit and a reduction of 3 percent occurs at high flow (Figure 14). Overall an increase of 8 percent of OR is found, consistent with expectations.

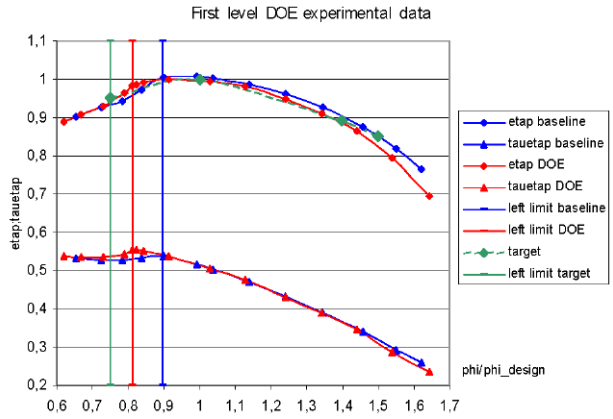

Figure 14. Experimental Validation of DOE.

The surge limit was improved from 89 percent to 82 percent; still less than targeted. Considering good results from previous CFD studies, two possible tracks were then considered to pursue the improvement of the impellers:

- Optimization of hub
- Introduction of splitter and heavier redesign of blade

Second Level—Hub DOE Optimization

Following good results from first optimization of the shroud, it was decided to apply the same strategy for hub optimization. Using the geometry from the shroud optimization as a new baseline, the same DOE based analysis was performed for hub curves (blue curves of Figure 10). As in the case of the shroud, indication of CFD gave, as most important parameter for range, the camber of the blade at leading edge.

CFD then identified a configuration with an expected additional improvement of 6 percent for the operating range. These studies were all based on numerical analysis of the impeller with perfect upstream inlet conditions.

Second Level DOE—Experimental Results

Experimental validation of this hub and a shroud-optimized impeller showed a strong downgrading of operating range. As the

test was done with a four airfoil configuration and CFD performed for the impeller alone, a decision was taken to:

- Compute the complete test rig configuration in order to take into account meridian flow distortions from upstream deswirl vanes.
- Experimentally test this impeller without upstream pre and deswirl vanes in order to suppress inlet secondary flows induced by the deswirl vane.

As shown by Figure 15, both tests and CFD "with distortion" confirmed that the last step of optimization was effectively better under perfect inlet conditions but, unfortunately, could not withstand flow distortions given by the deswirl vane.

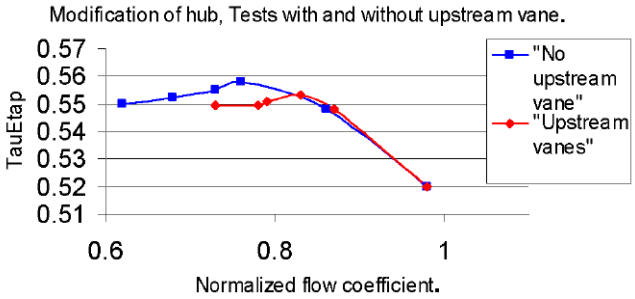

Figure 15. "Optimized" Hub Results, with and without Upstream Vanes.

Experimentally, surge limit was measured at 77.8 percent (first stage) and 85.9 percent (intermediate stage). Numerically, left limit was computed at 75.0 percent (first stage) and 83.1 percent (intermediate stage). Hub optimization phase had therefore missed this important factor and selected a design much too sensitive to distortions.

These results lead the authors to review CFD methodology in order to improve predictability and robustness of state-of-the-art design procedures (Horlock and Denton, 2005). In the meantime, it was decided to put in production a second generation of stages based on Shroud optimization only.

Improved CFD Methodology

Ideally, CFD would have to be performed, as for the test rig, in four airfoil configuration. Models to handle and time of computation would rise drastically. This is specifically true in the frame of an optimization related to range where whole speed-lines need calculation. An innovative solution called "two airfoils repeating" was defined and validated using available data, then implemented with internal software.

This solution allows computing standard stage configuration (impeller, vaneless diffuser, and deswirl vanes) while taking into account possible effects of flow distortions. This is done exporting stage exit distortions to stage inlet while still maintaining mean quantities.

The main idea for repeating stage methodology is based on the "normal stage" assumption, i.e., considering that stage inlet and outlet profiles are similar. Doing so, the user is not challenged with the task of providing realistic profiles to the impeller inlet (a profile that in a real compressor will change depending on design point) and stage exit. The inlet and outlet profiles are properly scaled to maintain the desired overall operating conditions while distortion of profile will change depending on operating point.

During all of the optimization phase, a big use of this two airfoil repeating methodology was done. Four airfoil methodology (Figure 16) is only used as a final step for direct comparison of CFD and test. It should be noted that in the test bench, and differently from a real compressor, impeller upstream flow distortion is quasi independent from the flow itself.

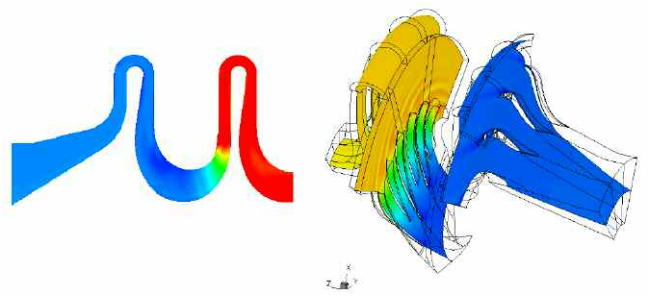

Figure 16. Four Airfoil Computational Domain and Geometries.

THIRD GENERATION OF STAGES

After results were obtained from the hub optimization, at least for the multistage configuration, attention was then focused on a solution with a more radical change. This was achieved with the addition and optimization of splitter blades still using the ruled surface approach.

Due to the radical change in configuration, a first screening was done on many parameters both with 1D correlations and different CFD codes. In this phase, the internal software repeating methodology was used for verification on some intermediate geometry. The main parameters investigated during this phase were:

- Meridional flow path.
- Design incidence angle.
- Splitter position centered or with azimuthal offset versus main blade.
- Bowed leading edge.
- Blade number optimization.

From this screening, little modification of the meridional flow path was done. Design incidences remained unchanged and bowed leading edge or splitter offset were not considered of sufficient interest. Optimization was, in the end, performed on the blade camber line and thickness plus splitter leading edge position.

In a way similar to the first modification, the new splitter design was in the direction of reducing the impeller loading in the leading edge portion, both at hub and shroud.

Before going to the test bench a last step of optimization and verification was done with this radically different design to optimize some mechanical aspects, check production constraints, and verify the possibility of deriving a family of stages in the desired range of flow coefficient. Similar designs were then created for flow coefficient 0.065 and 0.127 and have since been tested.

A shrouded impeller, with nine blades and nine splitters defined by ruled surfaces, characterizes this design (Figure 17) at flow coefficient 0.095. Vaneless diffuser and return channel with 16 deswirl vanes are left unchanged.

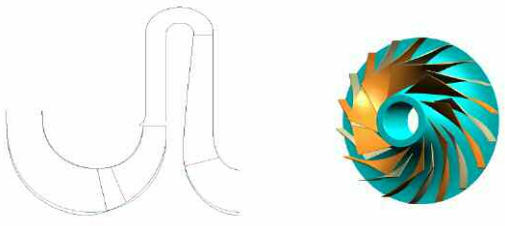

Figure 17. Splitter Design, Cross-Section Superimposed with Second-Generation Design and 3D, Unshrouded, Model.

CFD Investigation

While studies of first and second generation involved a variety of codes, in the last part of the optimization, the internal software was taken as the reference code with two airfoil repeating methodology. Best practices for use of this code in terms of meshing strategy and turbulence modeling are the ones derived from previous experience on 3D low Mach stages.

A final CFD validation of splitter versus second-generation design was done with four airfoil configuration to reproduce test rig geometries and the results obtained by the internal software are presented in Figure 18.

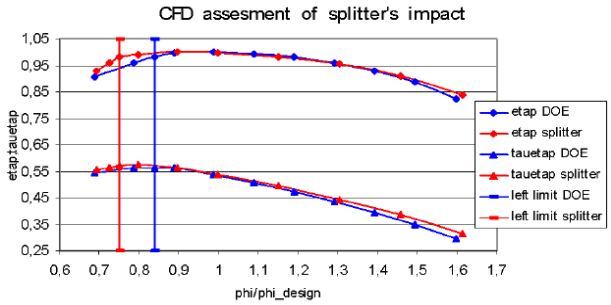

Figure 18. CFD Prediction of Splitter Versus Second-Generation.

A typical domain modeled for a four airfoil configuration is given in Figure 16. This helps us to appreciate why the calculation of a full speed-line during an optimization study has been judged inconvenient and that two airfoil repeating methodology has been preferred. Of course, qualification of two airfoil repeating methodology has been done comparing coherence of the two different types of calculation.

According to CFD results, both efficiency level and slope of TauEtap are improved to the left of operating range. This allows reaching 74 percent of design flow coefficient as left limit. Furthermore, CFD shows that the operating range to the left is now limited by stall inside the return channel. An estimation done for the operating range of the impeller alone (i.e., without downstream vanes) indicated an expected range of 67 percent.

Efficiency at the design point was estimated to be almost unaffected with a reduction of 0 to 1 percent affected mainly by splitter grid distortion.

Experimental Validation

Curves from experiments are given in Figure 19. Left limit was found at 75 percent and, interestingly, now with low frequencies (around 10 to 15 percent) more closely associated to a stall of a statoric component, either vaneless diffuser or deswirl vane. It appears that, in this case, CFD had also correctly captured stall coming from the deswirl vane. High frequency stall now appears in the range of 63 to 65 percent, also consistent with CFD indications for the impeller. Some operating range, around 2 to 3 percent, was also recovered at high flow.

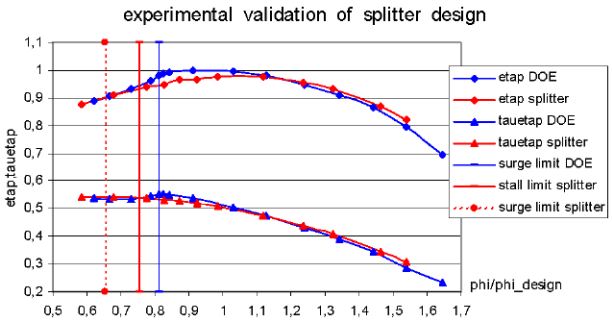

Figure 19. Experimental Curves.

Another observation concerns the significant change in the shape of the curve. Now a more rounded shape and maximum efficiency zone further away from the surge zone. Previously the maximum efficiency zone was located between the surge and design point, partly in the protection zone and therefore not possible to exploit. From a prediction point of view, it is observed that CFD did not capture the efficiency erosion that is found between the surge and design point with the latest generation.

Interestingly, the efficiencies of the generation two and generation three stages tend to converge after the impeller stall point of generation two. Primarily, the authors have replaced an abrupt stall at the leading edge with a much more progressive efficiency decay obtaining similar results when stall is fully developed. Efficiency of the third generation stage will be identical or better than the second generation one at 110 percent flow and higher, in the zone of maximum power where efficiency is even more important.

Considering the fact that the impeller is able to go down to much lower flow than the static components, one can also think that the impeller has been too “range optimized.” Considering what can be achieved with deswirl vanes, some intermediate step for the impeller could lead to a more coherent matching of rotor/stator at a reduced efficiency drop below 110 percent. For a single stage configuration with a well-adapted volute, a 65 percent operating range could be directly exploited.

Validation at Different Flow Coefficients

Third generation stages have been extended to design flow coefficients ranging from 0.065 to 0.127 using the same design tools and CFD verification. An experimental validation has been performed to check the behavior of this family as shown by Figures 20 and 21.

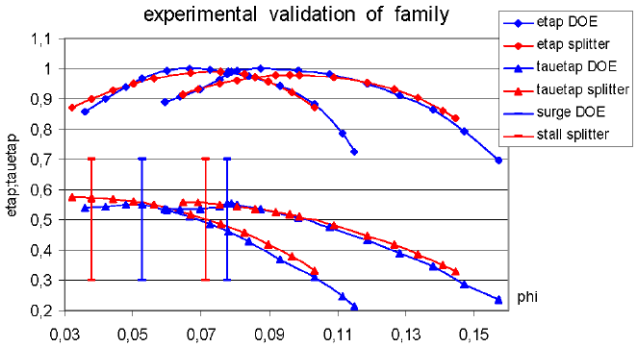

Figure 20. Third Versus Previous Generation Stages for Two Different Flow Coefficients.

Figure 21. Impeller of Third Generation for Flow Coefficient 0.127.

At a flow coefficient of 0.065, a comparison is done versus the first generation stage. Here again, some efficiency erosion can be seen offset by a spectacular 22 percent increase of operating range.

For the biggest flow coefficient, the test gave results similar to the one obtained at flow coefficient of 0.095 but no previous test was available for direct comparison.

ROTOR STATOR MATCHING— PRELIMINARY STATOR OPTIMIZATION

In the wake of this optimization of the impeller, similar work is now being conducted for deswirl vanes with the objective of achievable improvements in both operating range and/or loss coefficient for this component. Results of this study will then be used to identify best associations possible between rotor and stator with the idea to identify:

- A deswirl vane configuration having the same operating range as today with lower losses in order to compensate for impeller efficiency erosion.
- A configuration of deswirl vanes able to operate down to 65 percent to be coupled with the current version of impeller.

So far, test results are only partially available for the first option aimed at reducing deswirl vane losses at International Organization for Standardization (ISO) operating range.

As a way identical to the optimization done for the impeller, a first CFD screening has been performed, followed by optimization of the most important parameters identified:

- Vane counts
- Camber line evolution at leading edge
- Thickness evolution in leading edge zone

A fourth parameter investigated has been trailing edge angle, in order to exactly match targeted exit flow angle and suppress existing counter rotation. The DOE methodology followed was exactly the same as for the impeller.

The reason for investigating the impact of vane count in this case was mainly because, historically, criteria for deswirl vane blade loading had been much less precise than the one used for impellers without splitters. From this optimization, a configuration was identified having a 20 percent increase in vanes, 15 percent increase in blade thickness, and reduced leading edge curvature.

In Figure 22, a comparison of test results between baseline and optimized configuration is presented in terms of pressure recovery coefficient. These test results are showing quite a significant improvement, specifically at low flow where efficiency erosion from the third generation impeller is more pronounced.

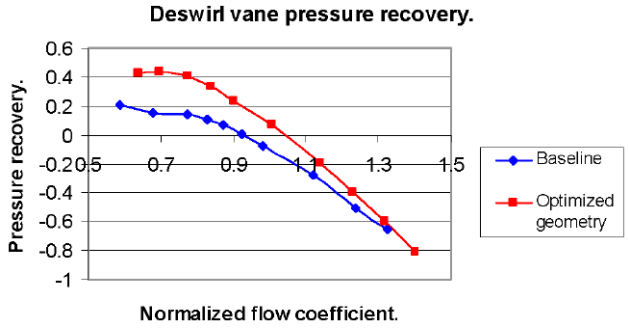

Figure 22. Comparison of Pressure Recovery Coefficient for Optimized and Baseline Deswirl Vanes.

Part of this increased pressure recovery coefficient comes from more radial flow (i.e., lower speed) and less distortion at stage exit. In the baseline configuration some overturning of the flow was present. The other part is linked to reduction of losses.

Overall, the optimized deswirl vane currently tested has allowed recovery of 1.5 pts with no modification of the operating range.

CONCLUSIONS

This study has demonstrated the usefulness of CFD based optimization with DOE techniques for improvement of impeller operating range and has been the opportunity to improve CFD strategy developing a two airfoil repeating stage methodology.

In some zones of the operating curve, efficiency erosion demonstrated by test was partly caught by CFD and experimental data are now available to allow quantifying the balance between efficiency and range. In fact, in the frame of this study, CFD has given rather small efficiency variations, either for impeller or deswirl vane design modifications, when compared to actual test results. A detailed assessment of the reason of this low efficiency sensitivity has been started as it could indicate that some phenomena need improved modeling.

Experimental evidence indicated the usefulness of CFD to estimate operating range of the impeller. Similar CFD based optimization strategies have given the first promising results for deswirl vane efficiency. Synthesis of efficiency variation and operating range are summarized in Table 2.

Table 2. Test Synthesis, Evolution of Operating Range, and Design Efficiency from Baseline.

Configuration	OR / OR baseline	Efficiency variation from baseline
Baseline	100%	0.0%
2nd generation - shroud	116%	-0.5%
2nd generation hub and shroud	103%	-0.7%
3rd generation	152%	-2.0%
3rd generation impeller and return channel.	152%	-0.5%
Target	150%	0.0%
Best possible solution*	150%	0.5%

* expected performances with 3rd generation impeller fine tuned and optimized return channel

Overall, a very precise optimization of rotor and stator components and of their matching can be achieved combining CFD with experiments. While the authors' best currently tested configuration has allowed them to reach a targeted operating range with a loss of 0.5 percent efficiency, the "best possible" solution could allow maintaining the targeted range and increasing slightly the best efficiency.

The first two generations of stages have already been used in commercial application and installed onsite. The third generation will be introduced during this year after completion of the testing phase on statoric components.

NOMENCLATURE

DOE = Design of experiment
Etap = Normalized polytropic efficiency
IOR = Impeller operating range
OR = Operating range
Phi = Flow coefficient
Q_v = Volume flow rate (ft^3/s)
R_2 = Impeller exit radius (ft)
Rpm = Round per minute
TauEtap = Polytropic head coefficient
Φ_{design} = Flow coefficient at design point = $\frac{30 * Q_v}{\pi^2 * \omega * R_2^3}$
Φ_{left} = Flow coefficient of left limit of operating range
Φ_{right} = Flow coefficient of conventional upper limit of operating range
η = Polytropic efficiency
η_{design} = Polytropic efficiency at design point
ω = Rotational velocity (rpm)

REFERENCES

Aungier, R. H., 2000, *Centrifugal Compressors: A Strategy for Aerodynamic Design and Analysis,* New York, New York: ASME Press, pp. 151-156.

Bonaiuti, D., Arnone, A., Ermini, M., and Baldassarre, L., 2006, "Analysis and Optimization of Transonic Centrifugal Compressor Impellers Using the Design of Experiments Technique," Journal of Turbomachinery, *128,* (4), pp. 786-797.

Dallenbach, F., 1961, "The Aerodynamic Design and Performance of Centrifugal and Mixed-Flow Compressors."

Horlock, J. H. and Denton, J. D., 2005, "A Review of Some Early Design Practice Using Computational Fluid Dynamics and a Current Perspective," Journal of Turbomachinery, *127,* (1), pp. 5-13.

Japikse, D., 1996, *Centrifugal Compressor Design and Performance,* Chapter 6, Wilder, Vermont: Concepts ETI.

Nishida-Nishina, 1983, "Effect of Relative Velocity Distribution on Efficiency/Exit Flow of Centrifugal Impellers," ASME.

NIST/SEMATECH e-Handbook of Statistical Methods, 2003, http://www.itl.nist.gov/div898/handbook/, U.S. Commerce Department, Washington, D.C.